Chemistry Research Journal, 2021, 6(3):132-138

Available online www.chemrj.org

Research Article

ISSN: 2455-8990
CODEN(USA): CRJHA5

Synthesis and Characterization of Mixed-Ligand Complexes Containing Isonid and Ethanolamine

Alaa E. Ali*, Gehan S. Elasala, Yasser Ramadan

Chemistry Department, Faculty of Science, Damanhour University, Egypt
*email address: Dralaae@yahoo.com

Abstract Synthesis, spectral characterization and thermal analysis of mixed ligand complexes with transition metals (Cr(III), Mn(II), Fe(III), Co(II), Ni(II), Cu(II), Zn(II), Cd(II) and Hg(II)) were discussed. Mixed ligands act as bidentate ligands with formation of 1:1:1 (M: L:L). Measurement of magnetism and spectral data shows octahedral structures for all complexes. Hyper chemistry program confirmed the binding sites of mixed ligand. Complexes show higher activity than commercial one for some strains.

Keywords Mixed ligand, ethanol amine Complexes, isonid complexes, biological activity

Introduction

Ethanolamine is a colorless, viscous liquid with an odor reminiscent of ammonia [1]. Its derivatives are widespread in nature; e.g., lipids, as precursor of a variety of N-acylethanolamines (NAEs), that modulate several animal and plant physiological processes such a seed germination, plantpathogen interactions, chloroplast development and flowering, [2] as well as precursor, combined with arachidonic acid ($C_{20}H_{32}O_2$; 20:4, ω-6), to form the endocannabinoid Anandamide (AEA: $C_{22}H_{37}NO_2$; 20:4, ω-6) [3]. The ethanolamines comprise a group of amino alcohols. A class of antihistamines is identified as ethanolamines, which includes carbinoxamine, clemastine, dimenhydrinate, Chlorphenoxamine, diphenhydramine and doxylamine.

Isoniazid, also known as isonicotinic acid hydrazide (INH), is an antibiotic used for the treatment of tuberculosis [1]. For active tuberculosis it is often used together with rifampicin, pyrazinamide, andeither streptomycin or ethambutol [2]. For latent tuberculosis it is often used by itself. Mixed-ligand transition metal complexes of some ions were synthesized and characterized.

Result and Discussion

Table (2) collected the IR spectra of the amino alcohol ligand. The bands due to ν_{OH}, δ_{OH}, δ_{NH}, γ_{OH} are assigned. The broadness of vibrations–OH is mainly due to strong intermolecular hydrogen bonds in the three ligands, while isonid ligand. The band at 1653 cm^{-1} in the spectrum of the ligand (isoniazid) is a characteristic of the C=O. This band underwent a shift to 1721 cm^{-1}, 1680 cm^{-1}, 1599 cm^{-1}, 1650 cm^{-1}. Numbers suggests the involvement of the amino nitrogen in the coordination to the metal ions.

The Cr – complexes coordination occurs through N atom which is indicates by red shift of δ_{NH} from 1160 cm^{-1} in free MEA to 1150 cm^{-1}, beside appearance of ν_{M-N} stretching at 535 cm^{-1} and ν_{M-O} at 429 cm^{-1}

While The Mn-complex coordination occurs through N atom which is indicates by red shift of δ_{NH} from 1160 cm^{-1} in free MEA to 1148 cm^{-1}, beside appearance of ν_{M-N} stretching at 530 cm^{-1} and ν_{M-O} at 424 cm^{-1} . The infra-red of Fe-complex coordination occurs through N atom which is indicates by red shift of δ_{NH} from 1160 cm^{-1} in free MEA to 1145 cm^{-1}, beside appearance of ν_{M-N} stretching at 530 cm^{-1} and ν_{M-O} at 424 cm^{-1} The Co-complexes coordination occurs through N atom which is indicates by red shift of δ_{NH} from 1160 cm^{-1} in free MEA to 1143 cm^{-1}, beside appearance of ν_{M-N} stretching at 421 cm^{-1} and ν_{M-O} at 376 cm^{-1}.

While the Ni-complex coordination occurs through N atom which is indicates by red shift of δ_{NH} from 1160 cm^{-1} in free MEA to 1140 cm^{-1}, beside appearance of ν_{M-N} stretching at 524 cm^{-1} and ν_{M-O} at 419 cm^{-1}. While the Cu-complex coordination occurs through N atom which is indicates by red shift of δ_{NH} from 1160 cm^{-1} in free MEA to 1155 cm^{-1}, beside appearance of ν_{M-N} stretching at 517 cm^{-1} and ν_{M-O} at 424 cm^{-1}.

The Zn-complexes coordination occurs through N atom which is indicates by red shift of δ_{NH} from 1155 cm^{-1} in free MEA to 1143 cm^{-1}, beside appearance of ν_{M-N} stretching at 515 cm^{-1} and ν_{M-O} at 410 cm^{-1}.

While The Cd-complex coordination occurs through N atom which is indicates by red shift of δ_{NH} from 1160 cm^{-1} in free MEA to 1078 cm^{-1}, beside appearance of ν_{M-N} stretching at 481 cm^{-1} and ν_{M-O} at 378 cm^{-1} and the Hg - complexes coordination occurs through N atom which is indicates by red shift of δ_{NH} from 1160 cm^{-1} in free MEA to 1147 cm^{-1}, beside appearance of ν_{M-N} stretching at 459 cm^{-1} and ν_{M-O} at 357 cm^{-1}.

Table 1: Fundamental infrared bands (cm^{-1}) of MEA, ISO and its metal complexes

IR	V_{OH}	δ_{CH2}	δ_{OH}	NH_2	V_{C-O}	T_{C-C}	δ_{NH}	γ_{M-N}	γ_{M-O}	γ_{M-Cl}
MEA	3435	1445	1609	1160	1120	980	1630	-	-	-
[Cr(MEA)(ISO)$(Cl)_2$]	3445	1480	1345	1150	733	1118	1625	535	429	344
[Mn(MEA)(ISO)(Cl)(H_2O)]	3441	1480	1340	1148	732	1115	1630	530	424	346
[Fe(MEA)(ISO)$(Cl)_2$]	3440	1479	1338	1145	733	1115	1633	533	426	348
[Co(MEA)(ISO)(Cl)(H_2O)]	3450	1480	1335	1143	733	1117	1625	421	367	343
[Ni(MEA)(ISO)(Cl)(H_2O)]	3450	1483	1354	1140	733	1117	1624	524	419	343
[Cu(MEA)(ISO)(Cl)(H_2O)]	3450	1448	1347	1155	730	1121	1579	517	412	344
[Zn(MEA)(ISO)(Cl)(H_2O)]	3400	1482	1551	1155	718	1125	1625	515	410	340
[Cd(MEA)(ISO)(Cl)(H_2O)]	3400	1480	1531	1078	716	1109	1626	481	378	339
[Hg(MEA)(ISO)(Cl)(H_2O)]	3400	1480	1552	1047	709	1129	1620	459	357	335

Electronic absorption spectra and magnetic susceptibility studies

Chromium-complexes

The electronic absorption spectra for the violet chromium-complexes, [Cr(MEA)(ISO)$(Cl)_2$] showed three bands at, 403, 570 nm due to $^4A_{2g}\rightarrow{}^4T_{2g}$ (F), $^4A_{2g}\rightarrow{}^4T_{1g}$(F) and $^4A_{2g}\rightarrow{}^4T_{1g}$(p) transitions, respectively,. So that, the complex have octahedral geometries. Such O_h geometry is further deduced from the μ_{eff} value which equal, 4.30 [3-4]. However, the Yellow electronic absorption spectrum of manganese-complexes[Mn(MEA)(ISO)(Cl)(H_2O)], Table (2), gave band 350 where the first band is assigned to $^6A_{1g}\rightarrow{}^4A_{1g}$, while the second is due to $^6A_{1g}\rightarrow{}^4T_{2g}$ transition and the last band is due to $^6A_{1g}\rightarrow{}^4T_{1g}$ transition [3-4]. Its room temperature μ_{eff} value of 5.99 B.M, respectively, typified the existence of O_h configuration. The brown electronic absorption spectra of iron-complexes, [Fe(MEA)(ISO)$(Cl)_2$] and Table 2, gave band at 343 nm, These bands are due to CT ($t_{2g} \rightarrow \pi^*$) . Its room temperature μ_{eff} value of 5.82 typified the existence of O_h configuration [5-6]. The electronic absorption spectra of[Co(MEA)(ISO)(Cl)(H_2O)], Table (2), gave bands at 430, 555, nm bands are assigned to $^4T_{1g}(F) \rightarrow {}^4T_{2g}(P)$ transition with magnetic moment value equal to 5.85 typified the existence of the complex in O_h geometry The green electronic absorption spectra for Nickel-complexes, [Ni(MEA)(ISO)(Cl)(H_2O)]showed three bands at 420, 545, 650 nm due to $^3A_{2g}\rightarrow{}^3T_{1g}(p)$, $^3A_{2g}\rightarrow{}^3T_{1g}$ (P) transitions, Table (2). So the complex have octahedral geometrie, further deduced from the μ_{eff} values which equal, (2.81) B.M The copper complexes[Cu(MEA)(ISO)(Cl)(H_2O)], Table (2), exhibited bands at 425 . 550 nm with μeff=1.41 B.M. The latter broad band is assigned to the $^2E_g \rightarrow {}^2T_{2g}$ (D) transition assignable to octahedral environment [7-8].

These complexes exhibited only a high intensity band at 343-426 nm, which are assigned to ligand →metal charge transfer. Owing to the d^{10}- configuration of Zn(II), Cd(II) and Hg(II), no d-d transition could be observed and therefore the strerochemistry around these metals in its complexes cannot be determined from ultraviolet and visible spectra. However, by comparing the spectra of these complexes and those of similar environments, a octahedral structures suggested for these complexes [9].

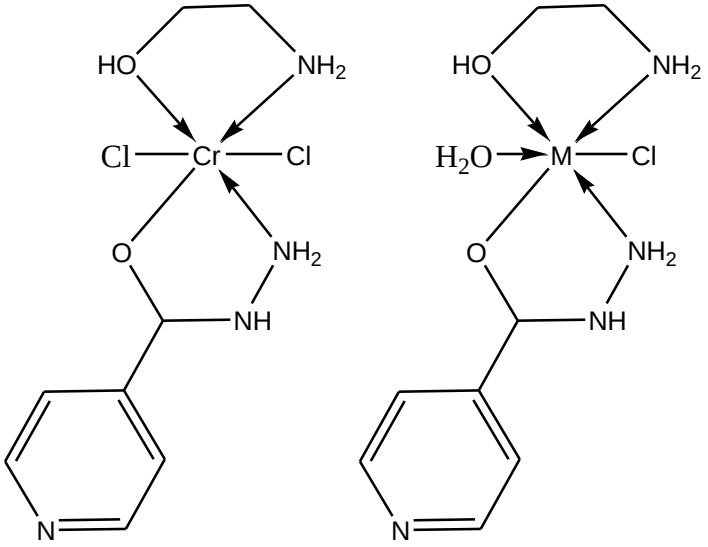

Table 2: Nujol mull electronic absorption spectra λ_{max} (nm), room temperature effective magnetic moment values (μ_{eff} 298°K) and geometries of mixed ligand metal complexes

Complex	λ_{max} (nm)	μ_{eff}	Geometry
$[Cr(MEA)(ISO)(Cl)_2]$	402, 570	4.30	O_h
$[Mn(MEA)(ISO)(Cl)(H_2O)]$	350	5.99	O_h
$[Fe(MEA)(ISO)(Cl)_2]$	343	5.82	O_h
$[Co(MEA)(ISO)(Cl)(H_2O)]$	430, 555	4.40	O_h
$[Ni(MEA)(ISO)(Cl)(H_2O)]$	420,545 .650	2.81	O_h
$[Cu(MEA)(ISO)(Cl)(H_2O)]$	425, 550	1.41	O_h
$[Zn(MEA)(ISO)(Cl)(H_2O)]$	426	diamagnetic	O_h
$[Cd(MEA)(ISO)(Cl)(H_2O)]$	337	diamagnetic	O_h
$[Hg(MEA)(ISO)(Cl)(H_2O)]$	343	diamagnetic	O_h

Thermal Analysis

The TGA and DTA data of $[Cr(MEA)(ISO)(Cl)_2]$and its complexes allow the following observations and conclusions:

From TGA thermo gram, $[Cr(MEA)(ISO)(Cl)_2(H_2O)]$decomposition occurs in several bonds at the same time due to it is highly branched. From DTA curve, $[Cr(MEA)(ISO)(Cl)_2]$ decomposition occurs in three steps at 94.4, 453 and 554 ºC respectively with activation energies 6.34, 294.4, 158.77 and 47.02 KJ/mole with orders. All orders are of the first type except the third one is of the second order type. This can be proved by TGA data which gave well defined four peaks, so that the decomposition equation may be supposed as follows in scheme (1). On the other hand, the DTA data of $[Mn(MEA)(ISO)(Cl)(H_2O)]$, complex showed three peaks, at 118.8, 181.3, 272.5, and 550.4°C with activation energies 11.7, 81.6, 82.48, and 240,66 kJ/mole, respectively. The orders of reactions were 1.23, 1.3609,

0.77, and 1.95, respectively. All peaks are of the first order type except the fourth peaks are second order type. Only the second peak is endothermic type while the other peaks are exothermic types [10-11].

This can be proved by TGA data which gave well defined four peaks, scheme (2):

However, the Nickel complex[Ni(MEA)(ISO)(Cl)(H_2O)], showed three peaks at 102.3, 197.1 ,268.5.5 and 340°C with activation energies 24.04, 31.68 , 66.05 and 77.05 kJ/mole, respectively and the orders of reactions are first order. All peaks are exothermic except the second one is endothermic. The TGA data confirmed these results which it gave three peaks, scheme (3):

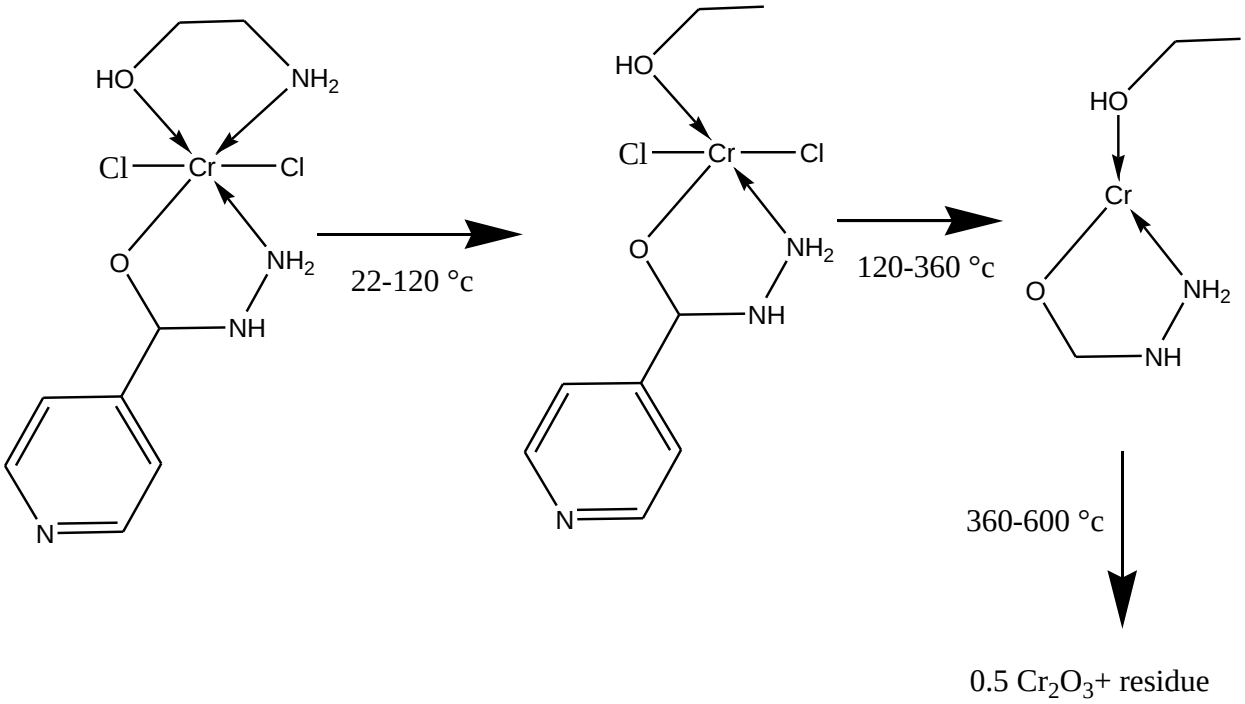

Scheme 1: Thermolysis of [Cr(MEA)(ISO)(Cl)$_2$]

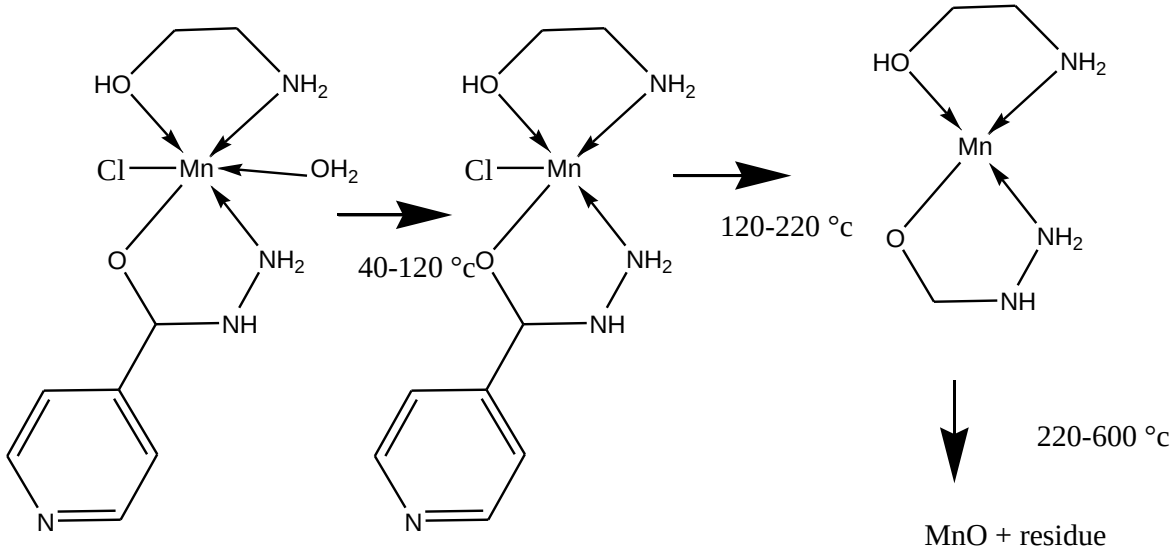

Scheme 2: Thermolysis of [Mn(MEA)(ISO)(Cl)(H_2O)]

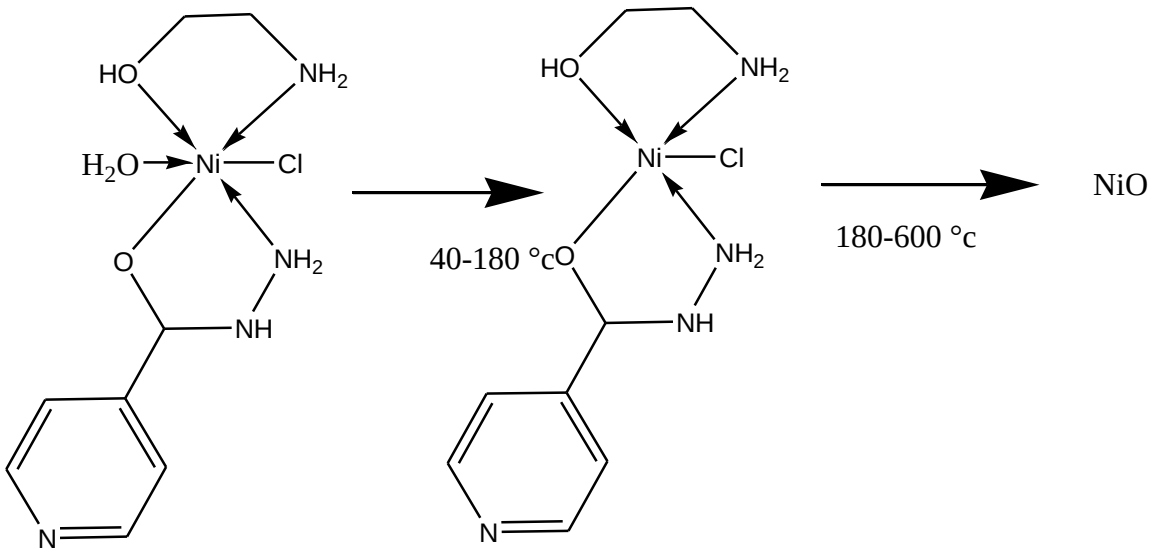

Scheme 3: Thermolysis of [Ni(MEA)(ISO)(Cl)(H_2O)]

ESR

Complex	**G**	**g_s**	**$g_{\|}$**	**$g_{\perp}$**	**<g>**	**g_1**	**g_2**	**g_3**	**R**	**$A_{//}$**	**$A_{\perp}$**	**|A|**	α^2	**F^2**
[Cu(MEA)(ISO)(Cl)(H_2O)]	4.4		2.66	1.83	2.12					130×10^{-4}	22×10^{-4}	5.2×10^{-3}	0.985	1.230

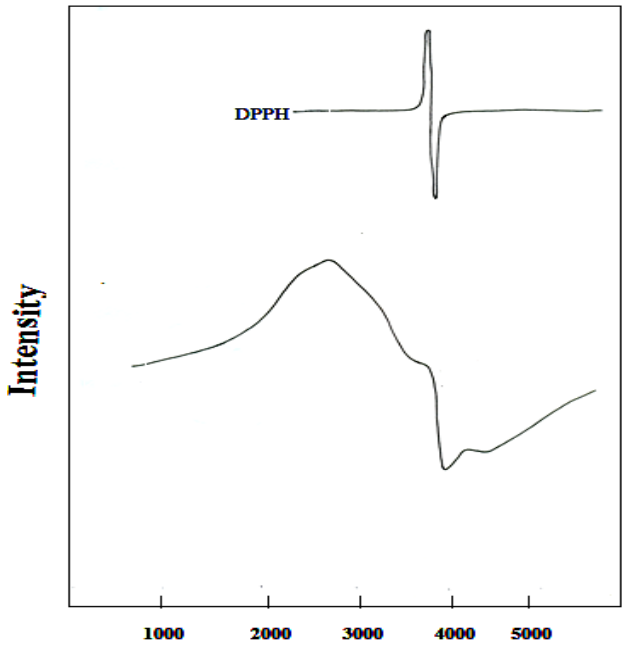

The presence of a typical ligands introduces 4s character in the ground state which decreases the contact hyper fine interaction. Therefore, if the 4s character in the ground state is known, it is possible to know the axial field strength in the presence of small percentage of 4s character in the ground state, the fraction of the 3d character in the Cu^{II} 3d-4s ground state, F^2, can be determined from the following equation [12-16]:

$$\alpha^2 F^2 = 7/4 [A_{\|} / 0.036 - A / 0.036 + 2/3 g_{\|} - 5/21 g_{\perp} - 6/7]$$

Where $A = 6/15\ A_{\|}$

The value of α^2 for[Cu(MEA)(ISO)(Cl)(H_2O)] complex is 0.985, assigns that Cu-O bond is more pronounced than the Cu-N bonding,

Biological Activity

In this study, 5 microorganisms representing different microbial categories, {three Gram-positive (*Staphylococcus aureas*, *Streptococcus penumonia* and *Bacillus subtilis*), two Gram negative (*Escherischia colistrain* and *Pseudomonas aeruginosa*) bacteria were used.

All the investigated compounds have higher positive antibacterial activity compared to antifungal activity. Mn, Zn, Co–complexes shows higher activity in all microbial categories while Fe –complex shows a good result in *Streptococcus penumonia* and *Bacillus subtilis* and no activity for other microbial categories and Ni complex show a higher activity in all microbial categories except for *Staphylococcus aureas*.

Most of the metal complexes have higher activity [17-20] than the free ligands such increased activity of the metal chelates could be explained on the bases of overtone's concept and chelation theory [19, 24]. The cell permeability the lipid membrane that surrounds the cell favours the passage of only lipid soluble materials on the basis that liposolubility is an important factor that controls antimicrobial activity. On chelation, the polarity of the metal ion is reduced to a greater extent due to the overlap of the ligand orbital and partial sharing of the positive charge of the metal ion with the donor groups. Further, it increases the delocalization of p- and d-electrons over the whole chelate and enhances the lipophilicity of the complex. The increased lipophilicity enhances the penetration of the complexes into lipid membranes and blocking of metal binding sites on the enzymes of the microorganism.

Table 3: Antimicrobial activity of investigated complexes

		Mn	**Fe**	**Co**	**Ni**	**Zn**
Gram Positive	*Bacillus subtilis*	+++	+	++	+	+
Bacteria	*Streptococcus penumonia*	++	++	+++	++	+++
	Staphylococcus aureas	+++	-	+	-	++
Gram Negative	*E. coli*	+	+	+++	+	+++
Bacteria	*Pesudomonas* Sp.	++	-	+	+	+++
Antifungal Activity	*Candida*	+	-	+	-	++
	Aspergillus Niger	++	-	+++	++	+++
	Penicillium Sp.	+++	-	++	+++	++

Note:

(-) No clearing zone; inactive. (++) Medium clearing zone; moderately active.

(+) Small clearing zone; slightly active. (+++) Large clearing zone; highly active.

Reference

[1]. Andreani J, Le Bideau M, Duflot I, Jardot P, Rollanda C, Boxberger M, et al. In vitro testing of hydroxychloroquine and azithromycin on SARS-CoV-2 shows synergistic effect. Microb Pathog. 2020; 25(145):104228. doi: 10.1016/j.micpath.2020.104228.

[2]. Gautret P, Lagier JC, Parola P, Hoang VT, Meddeb L, Mailhe M, et al. Hydroxychloroquine and azithromycin as a treatment of COVID-19: results of an open-label non-randomized clinical trial. Int J Antimicrob Agents. 2020 doi: 10.1016/j.ijantimicag.2020.105949.

[3]. Andreani J, Le Bideau M, Duflot I, Jardot P, Rollanda C, Boxberger M, Bou Khalil JY, Baudouin JP, Wurtz N, Rolain JM, Colson P, La Scola B, Raoult D. In vitro testing of hydroxychloroquine and azithromycin on SARS-CoV-2 shows synergistic effect. 2020.

[4]. Yao X, Ye F, Zhang M, Cui C, Huang B, Niu P, et al. In vitro antiviral activity and projection of optimized dosing design of hydroxychloroquine for the treatment of Severe Acute Respiratory Syndrome Coronavirus 2 (SARS-CoV-2) Clin Infect Dis. 2020 doi: 10.1093/cid/ciaa237.

[5]. Ye Q, Wang B, Mao J. The pathogenesis and treatment of the 'cytokine storm' in COVID-19. J Infect. 2020; 80: 607–613. doi: 10.1016/j.jinf.2020.03.037.
[6]. Tran DH, Sugamata R, Hirose T, Suzuki S, Noguchi Y, Sugawara A, et al. Azithromycin, a 15-membered macrolide antibiotic, inhibits influenza (H1N1)pdm09 virus infection by interfering with virus internalization process. J Antibiot (Tokyo). 2019; 72: 759–768. doi: 10.1038/s41429-019-0204-x
[7]. Kostova I (2010) Metal-containing drugs and novel coordination complexes in therapeutic anticancer applications-part II. Anticancer Agents Med Chem 10:352 353
[8]. Masoud M.S., Ali A.E., Elasala G.S., kolkaila S.A. Synthesis, spectroscopic, biological activity and thermal characterization of ceftazidime with transition metals, Spectrochim. Acta., 193, (2018) 458-466
[9]. Masoud M.S., Ali A.E., Elasala G.S., kolkaila S.A., spectroscopic studies and thermal analysis on cefoperazone metal complexes, J. Chem. Pharm. Res. 9, (2017) 171-179.
[10]. Ali A. E. , Elasala G. S., Mohamed E. A., kolkaila S.A.,Spectral, thermal studies and biological activity of pyrazinamidecomplexes, heliyon, 5(11), (2019).
[11]. Ali A. E., Elasala G. S., Mohamed E. A. kolkaila, S.A., J. materials today proceeding https://doi.org/10.1016/j.matpr.2020.12.403 (2021).
[12]. Masoud M.S., Ali A.E., Elasala G.S., sakr S.F, kolkaila S.A.,Structural, J. Chem. Pharm. Res. 12, (2020) 42-52.
[13]. Masoud M.S., Ali A.E., Elasala G.S., sakr S.F, kolkaila S.A.,J. Chem. Pharm. Res. 12, (2020) 29-41.
[14]. Lee R.H, Griswold E. and Kleinberg J., Inorg. Chem. 3 (1964)1278-1283
[15]. Vogel A.I, A Text Book of Quantitative Inorganic Analysis, Longmans, London, (1989) 722-726.
[16]. Sher A, Rau H, Greiner G, Haubold W (1996) Spectroscopic and polarographic investigations of copper(II)-azithromycin interactions under equilibrium conditions. International Journal of Pharmaceutics 133: 237-244.
[17]. Howlader M.B.H., Islam M.S. and Karim M. R., J. Chem., 39 A, (2000) 407-409.
[18]. Atkins R, Brewer G, Kokot E, Mockler G. M and Sinn E, Inorg. Chem, 24, (1985) 127.
[19]. Krishnamoorthy C. R.and Taquikhan M. M,J. Coord. Chem, 12(4), (1983) 313.
[20]. Kirubavathy S. J, Velmurugan R, Parameswari K and Chitra S, IJPSR., 5(6), (2014) 2508-2517.
[21]. Luke, D.R.; Foulds, G. Disposition of oral azithromycin in humans. Clin. Pharmacol. Ther., 61(6), (1997), 641-648.
[22]. Li, H.; Liu, S.M.; Yu, X.H.; Tang, S.L.; Tang, C.K. Coronavirus disease (COVID-19): Current status and future perspectives. Int. J. Antimicrob. Agents, (2019).
[23]. Te. Velthuis, A.J.W.; van den Worm, S.H.E.; Sims, A.C.; Baric, R.S.;Snijder, E.J.; van Hemert, M.J. Zn(2+) inhibits coronavirus and arterivirus RNA polymerase activity in vitro and zinc ionophores block the replication of these viruses in cell culture. PLoS Pathog., 6(11), (2010) e1001176.
[24]. Bernabeu, C.; Tobin, E.M.; Fowler, A.; Zabin, I.; Lake, J.A. Nascentpolypeptide chains exit the ribosome in the same relative position in both eucaryotes and procaryotes. J. Cell Biol, 96(5), (1983) 1471-1474.